Scientific Papers of
the Institute of Electrical Power Engineering of
the Wrocław University of Technology

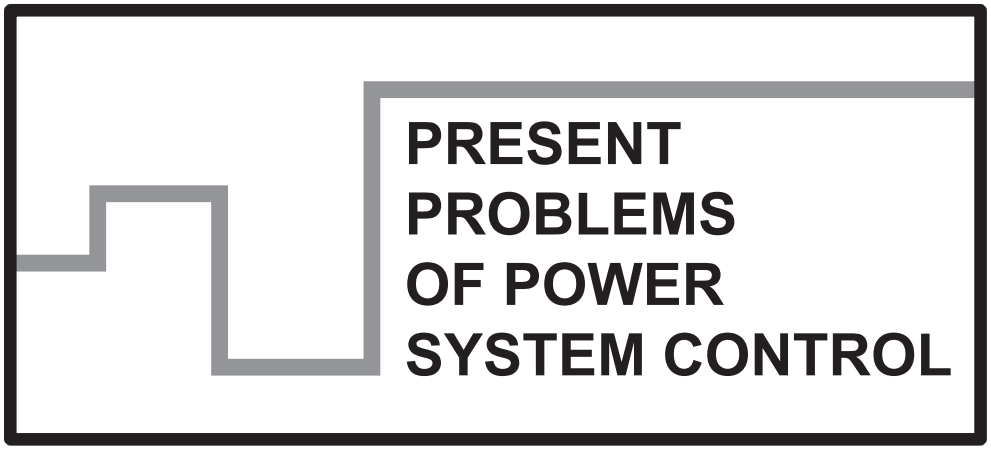

3

Wrocław 2013

Printed in the camera ready form

Institute of Electrical Power Engineering
Wrocław University of Technology
Wybrzeże Wyspiańskiego 27, 50-370 Wrocław, Poland
phone: +48 71 320 26 55, fax: +48 71 320 26 56
www: http://www.ie.pwr.wroc.pl/; e-mail: Inst.Energ@pwr.wroc.pl

OFICYNA WYDAWNICZA POLITECHNIKI WROCŁAWSKIEJ
Wybrzeże Wyspiańskiego 27, 50-370 Wrocław
http://www.oficyna.pwr.wroc.pl
e-mail: oficwyd@pwr.wroc.pl
zamawianie.ksiazek@pwr.wroc.pl

ISSN 2084-2201

Drukarnia Oficyny Wydawniczej Politechniki Wrocławskiej. Order No. 295/2013.

arc fault,
fault location,
signal processing

Mateusz PUSTUŁKA*, Jan IŻYKOWSKI*,
Mirosław ŁUKOWICZ*

LOCATION OF ARC FAULTS ON POWER TRANSMISSION LINES

This paper presents a fault location algorithm, which allows to determine the distance to a fault and fault resistance, as a result of considering natural fault loops. It is assumed that three-phase voltages and currents from both ends of the line measured asynchronously are the input signals of the fault locator. In case of the availability of synchronized measurements the elements associated with the determination of the synchronization angle should be omitted. In addition to natural fault loop signals also use of symmetrical components (positive and negative or incremental positive sequence components) to fault location were considered as well.

1. INTRODUCTION

The reliable operation of the electric power grid is one of the main goals of power system operators. Reduction of the duration of outages is one of the key requirements. There are many different ways that this goal can be achieved, with accurate fault location for an inspection-repair purpose [1]–[4] being one of them.

Algorithms for accurate location of faults on power lines have been a subject of great interest of researchers since the power system reliability became an important factor for network operators and customers [3]. Among the known methods, the approach based on an impedance principle is the most popular and most frequently implemented into protective relays or stand alone fault locators. In particular, the algorithms utilizing one-end current and voltage measurements have been introduced at the beginning [4]. Then two-end fault location principle [1]–[3] has been extensively explored. This principle is considered in the paper.

* Institute of Electrical Power Engineering, Wrocław University of Technology, Wrocław, Poland.

2. FAULT LOCATION ALGORITHM

Natural fault loops, identical as for a distance protection [2], are considered. For this purpose, the relaying signals (both voltage and current fault loop signals) are formed accordingly to the fault type. Table 1 defines those signals to any consideration of fault loops seen from the S end of the line for a single-circuit line (Fig. 1). Signals for fault loop seen from the R end are composed analogously.

In a case of phase-to-earth fault the voltage and current of a given faulted phase are taken, but the component associated with the zero-sequence component: zero-sequence current ($\underline{I}_{S0}$) multiplied by the factor: $k_0 = (\underline{Z}_{0L} - \underline{Z}_{1L})/\underline{Z}_{1L}$ is added to the phase current. This results from the fact that the impedances of the line for the positive sequence ($\underline{Z}_{1L}$) and zero sequence ($\underline{Z}_{0L}$) are not identical, and the impedance of the line section between the measuring point (S) and the fault point (F) for the positive sequence ($d\underline{Z}_{1L}$) is a measure of the distance to fault (d (p.u.)) – Fig. 1.

For a fault loop phase$_1$-to-phase$_2$, the differences of voltages and currents from the phases involved in the fault, respectively, are taken as the fault loop signals. As a result of the subtraction, the zero sequence component is eliminated and there is no compensation due to different line impedances for the positive and zero sequences.

Figure 1 shows the models of the considered fault loops (Fig. 1a, b) and the aggregated model (Fig. 1c).

Table 1. Composition of fault loop voltage and current signals for single-circuit line

Fault type	Fault loop voltage	Fault loop current
L1–E	$\underline{V}_{S\_L1}$	$\underline{I}_{S\_L1} + \underline{k}_0 \underline{I}_{S0}$
L2–E	$\underline{V}_{S\_L2}$	$\underline{I}_{S\_L2} + \underline{k}_0 \underline{I}_{S0}$
L3–E	$\underline{V}_{S\_L3}$	$\underline{I}_{S\_L3} + \underline{k}_0 \underline{I}_{S0}$
L1–L2, L1–L2–E, (L1–L2–L3, L1–L2–L3–E)*	$\underline{V}_{S\_L1} - \underline{V}_{S\_L2}$	$\underline{I}_{S\_L1} - \underline{I}_{S\_L2}$
L2–L3, L2–L3–E	$\underline{V}_{S\_L2} - \underline{V}_{S\_L3}$	$\underline{I}_{S\_L2} - \underline{I}_{S\_L3}$
L3–L1, L3–L1–E	$\underline{V}_{S\_L3} - \underline{V}_{S\_L1}$	$\underline{I}_{S\_L3} - \underline{I}_{S\_L1}$
* – includes loop L1–L2, but also loops L2–L3, L3–L1 can be analyzed, $\underline{k}_0 = \dfrac{\underline{Z}_{0L} - \underline{Z}_{1L}}{\underline{Z}_{1L}}$.		

Fault loop seen from the S end (Fig. 1a) consists of a line section of the positive sequence impedance: $d\underline{Z}_{1L}$ and the transverse branch that represents a fault (resistance: R_{arc}). In case of the fault loop seen from the R end (Fig. 1b) impedance of the line section for the positive sequence is: $(1 - d)\underline{Z}_{1L}$ and the transverse branch is as in the previous fault loop (Fig. 1a).

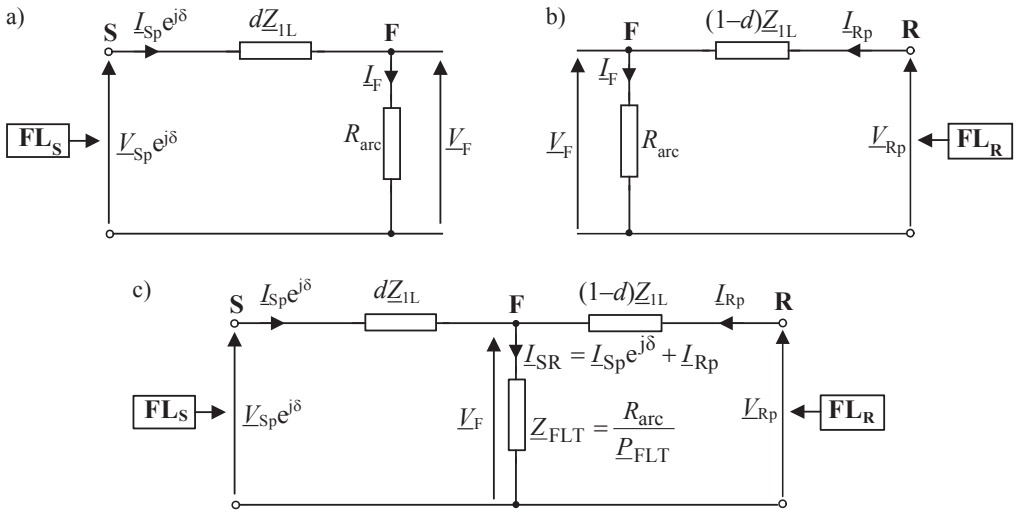

Fig. 1. Models of fault loop measurement for:
a) relay at bus S, b) relay at bus R, c) aggregated model

Use of unsynchronized measurements from both ends of the line is considered and the measurements from the R end (fault loop voltage and current: $\underline{V}_{Rp}$, $\underline{I}_{Rp}$) are assumed as a reference base. Therefore, the measurements from the S end (fault loop voltage and current: $\underline{V}_{Sp}$, $\underline{I}_{Sp}$) are synchronized analytically with use of the synchronization operator: $e^{j\delta}$, where δ – unknown synchronization angle. This is achieved by multiplying the phasors of the original fault loop signals of the bus S by this operator.

Aggregating both fault loop models from Fig. 1a and b leads to the model as shown in Fig. 1c [2]. There is a fictitious transverse branch, through which flows the total current ($\underline{I}_{Sp}\, e^{j\delta} + \underline{I}_{Rp}$) and not, as in reality: $\underline{I}_F$. Therefore, to provide the voltage in this branch: $\underline{V}_F$, as it is present in reality, the impedance of this fictitious branch ($\underline{Z}_{FLT}$) is not equal to the fault path resistance (R_{arc}). This impedance ($\underline{Z}_{FLT}$) matches the arc resistance (R_{arc}) divided by the complex factor: $\underline{P}_{FLT}$, which depends on the type of a fault (Table 2) [2].

Table 2. Coefficient $\underline{P}_{FLT}$ for different fault types

Fault type	$\underline{P}_{FLT}$
L1–E, L2–E, L3–E	$\frac{2\underline{Z}_{1L} + \underline{Z}_{0L}}{3\underline{Z}_{1L}}$
L1–L2, L2–L3, L3–L1	2
L1–L2–E, L2–L3–E, L3–L1–E, L1–L2–L3, L1–L2–L3–E	1

Comparison of voltage on the transverse branch, i.e. at the fault point (F) – determined from the S and R line ends (Fig. 1), respectively, yields:

$$\underline{V}_{\mathrm{Sp}}\mathrm{e}^{j\delta} - d\,\underline{Z}_{1\mathrm{L}}\,\underline{I}_{\mathrm{Sp}}\mathrm{e}^{j\delta} = \underline{V}_{\mathrm{Rp}} - (1-d)\underline{Z}_{1\mathrm{L}}\,\underline{I}_{\mathrm{Rp}} \tag{1}$$

Equation (1) can be written separately for the real and imaginary parts. This gives a system of two equations with two unknowns: d – fault distance (p.u.), δ – synchronization angle. It can be solved using very well-known numerical procedures. However, one may face problems with obtaining a correct solution. In fact, the unknowns are: d, $\sin(\delta)$, $\cos(\delta)$ while the synchronization angle δ can be positive or negative, i.e. in the following range: $-\pi <= \delta <= \pi$. Only one solution, out of two, is a correct one.

In order to avoid iterative calculations it is proposed to specify the modulus (absolute value) for the synchronization operator $\mathrm{e}^{j\delta}$ determined from (1) as follow:

$$\left|\mathrm{e}^{j\delta}\right| = \left|\frac{\underline{V}_{\mathrm{Rp}} - \underline{Z}_{1\mathrm{L}}\,\underline{I}_{\mathrm{Rp}} + d\,\underline{Z}_{1\mathrm{L}}\,\underline{I}_{\mathrm{Rp}}}{\underline{V}_{\mathrm{Sp}} - d\,\underline{Z}_{1\mathrm{L}}\,\underline{I}_{\mathrm{Sp}}}\right| \tag{2}$$

This gives:

$$\left|\underline{V}_{\mathrm{Rp}} - \underline{Z}_{1\mathrm{L}}\,\underline{I}_{\mathrm{Rp}} + d\,\underline{Z}_{1\mathrm{L}}\,\underline{I}_{\mathrm{Rp}}\right| = \left|\underline{V}_{\mathrm{Sp}} - d\,\underline{Z}_{1\mathrm{L}}\,\underline{I}_{\mathrm{Sp}}\right| \tag{3}$$

After tedious manipulations on (3) the following quadratic equation for the sought distance to fault is obtained:

$$A_2 d^2 + A_1 d + A_0 = 0 \tag{4}$$

where: A_2, A_1, A_0 – coefficients (real numbers) specified by the phasors of fault loop signals: ($\underline{V}_{\mathrm{Sp}}$, $\underline{I}_{\mathrm{Sp}}$) and ($\underline{V}_{\mathrm{Rp}}$, $\underline{I}_{\mathrm{Rp}}$), obtained with unsynchronized measurements at both ends of the line, and by the impedance of the line for the positive sequence ($\underline{Z}_{1\mathrm{L}}$), as follows:

$$A_2 = \left|\underline{Z}_{1\mathrm{L}}\,\underline{I}_{\mathrm{Sp}}\right|^2 - \left|\underline{Z}_{1\mathrm{L}}\,\underline{I}_{\mathrm{Rp}}\right|^2 \tag{5}$$

$$A_1 = -2\mathrm{real}[\underline{V}_{\mathrm{Sp}}(\underline{Z}_{1\mathrm{L}}\,\underline{I}_{\mathrm{Sp}})^* + (\underline{V}_{\mathrm{Rp}} - \underline{Z}_{1\mathrm{L}}\,\underline{I}_{\mathrm{Rp}})(\underline{Z}_{1\mathrm{L}}\,\underline{I}_{\mathrm{Rp}})^*] \tag{6}$$

$$A_0 = \left|\underline{V}_{\mathrm{Sp}}\right|^2 - \left|\underline{V}_{\mathrm{Rp}} - \underline{Z}_{1\mathrm{L}}\underline{I}_{\mathrm{Rp}}\right|^2 \tag{7}$$

where: $\underline{X}$* denotes conjugate of $\underline{X}$.

The solution of (4) gives two results for the sought fault distance (d_1, d_2). At least one of them indicates a detected fault in the line. If only one solution is such that it is satisfied: $0 < (d_1 \text{ or } d_2) < 1$, then in a natural way this solution is taken as the correct (valid). On the other hand, if it is obtained that the two solutions indicate a fault in the line: $0 < (d_1 \text{ and } d_2) < 1$, an additional selection of a solution that is correct has to be performed. Determination of the correct solution, which corresponds to the actual fault, can be determined by analyzing the estimated fault path resistance (in a general case it is obtained as the complex impedance). For the correct solution it should be very close to a pure resistance i.e. containing the smallest possible imaginary part.

As the input signals of the fault locator also symmetrical components of voltages and currents from both ends of the lines can be used:

- positive and negative – for asymmetrical faults,
- positive and incremental positive – for symmetrical three-phase faults.

In this case one needs replacing the fault loop signals in the derived equations (4)–(7) by the corresponding symmetrical components.

3. ARC FAULT LOCATION ANALYSIS

Fault location algorithm was performed using the signals generated by simulating arc faults [1] on the transmission line: 400 kV, 50 km with the aid of ATP-EMTP software. The representative results for the single-phase arc fault: *L*1–*E* are presented further.

Table 3 presents results when the fault loop signals are taken as the input signals, and Table 4 while positive and negative sequence components of voltages and currents from both ends of the line are applied. Both cases include the measurements acquired asynchronously – phasors of signals from the S end were software delayed by 15°, and thus the sought synchronization angle was $\delta = 15°$.

Standard full-cycle Fourier filtration was used as the basic in the considered location algorithms. It has been found that in some cases (rows in Table 3 marked with a shading), the applied filtering alone appears as insufficient due to a severe distortion of the processed signals. This is particularly in relation to the synchronization angle which is determined inaccurately. It was shown that performing the averaging of the results of the location in the fourth cycle after the fault, instead of averaging in the third cycle, significantly improves accuracy. Of course, this is possible only if the fault is not switched off earlier. An alternative approach to this is based on introducing

an additional pre-filtering, leaving the averaging within the 3rd cycle – as was assumed at the beginning of the study. Additional pre-filtration was used with half-cycle sine filter. It has been found that such extra pre-filtering contributes to a significant improvement of the fault location accuracy.

Selection of the correct solution out of the two obtained from the quadratic equation (4) was performed as follows: Table 3 – the correct solution is determined by taking the solution for which the estimated fault-path impedance has less imaginary part; Table 4 – only one of the solutions for the fault distance indicates a fault in the line and it is naturally assumed to be the correct solution.

Table 3. Arc location using fault loop signals

Accurate fault distance [km]	d_1 [km]	R_{arc1} [Ω]	δ_1 [°]	d_2 [km]	R_{arc2} [Ω]	δ_2 [°]	Error [%]
Full-cycle Fourier filtering Averaging within the third period after fault							
5.06	5.12	0.60 + 0.13i	17.41	6.30	0.59 + 0.22i	81.06	0.12
10.11	9.59	0.72 + 0.21i	–2.62	14.15	0.56 + 1.21i	137.50	1.04
17.52	17.36	0.96 + 0.25i	15.55	22.32	0.80 + 1.27i	139.63	0.32
22.22	22.12	0.69 + 0.18i	10.27	12.32	0.167 – 2.85i	–140.22	0.20
28.03	28.04	0.67 + 0.17i	16.66	31.68	0.71 + 0.90i	142.52	0.03
30.43	29.95	0.66 + 0.21i	–4.35	32.49	0.57 + 0.66i	113.53	0.95
35.59	35.65	1.60 + 0.39i	15.18	21.22	1.31 – 4.40i	–102.78	0.13
40.44	40.51	1.01 + 0.27i	16.38	27.96	1.23 – 3.85i	–105.03	0.14
45.75	45.74	0.36 + 0.08i	14.36	45.04	0.31 – 0.26i	–41.49	0.02
Full-cycle Fourier filtering Averaging within the fourth period after fault							
10.11	10.07	0.57 + 0.15i	14.87	13.63	0.59 + 0.91i	144.48	0.09
30.43	30.54	0.55 + 0.10i	21.38	31.98	0.56 + 0.30i	99.69	0.23
(Full-cycle Fourier filtering) + (Pre-filtration: sine half-period), Averaging within the third period after fault							
10.11	10.14	0.52 + 0.14i	17.19	13.57	0.59 + 0.87i	148.32	0.06
30.43	30.48	0.53 + 0.16i	12.69	32.14	0.49 + 0.38i	108.20	0.10

Table 4. Arc fault location using symmetrical component signals

Accurate fault distance [km]	Location for positive sequence		Location for negative sequence	
	d [km]	Error [%]	*d* [km]	Error [%]
5.06	4.86	3.88	5.15	1.76
10.11	9.94	1.68	9.80	3.11
17.52	17.40	0.69	17.16	2.03
22.22	22.16	0.25	22.14	0.38
28.03	28.04	0.03	28.04	0.02
30.43	30.48	0.17	30.24	0.64
35.59	35.88	0.81	34.78	2.27
40.44	40.71	0.67	40.32	0.30
45.75	45.85	0.23	46.17	0.91

Better accuracy was achieved by using fault loop signals and it is slightly better than the location with using of the measured data from one end of the line (Takagi algorithm [4]). This is the effect that in case of measurements at one end only (Takagi algorithm [4]), as a result of insufficient information there is a need for introducing simplifying assumptions.

4. CONCLUSION

Arc fault location on transmission lines with use of voltage and current measurements from both ends of the line acquired asynchronously has been considered. The derived algorithm applies the fault loop signals from the two ends of the line as the fault locator inputs. Quadratic equation for the sought distance to fault, whose coefficients are expressed in the most compact form, has been obtained. The selection of the correct solution (out of the two) is obtained by taking the solution for which the estimated impedance of the fault path has less imaginary part.

The derived algorithm can also be applied when symmetrical components of measured voltages and currents are applied as the locator input signals. One should then use: positive and negative sequence components for asymmetrical faults and positive and incremental positive sequence for three-phase symmetrical faults. For a correct solution there is a coincidence of the results obtained for two different components, which in practice means that they are very close to each other, while for the other solution (to be rejected) there are significant differences.

The results of the study indicate the important role of digital filtering of the processed signals that are severely distorted under arc faults. It is reasonable to take a direct result of the calculations or results averaged – as late as possible after fault incipience, but before its elimination. It has been shown that using the standard full-cycle Fourier filtering combined with the pre-filtering in the form of a half-cycle sine filter

improves considerably the accuracy of the calculation results. In particular, this relates to determining the synchronization angle.

Analyzed application of measurements from both sides of the line to fault location does not require introducing the simplifying assumptions, which are necessary if the location is performed with only the local measurements. As a result, better accuracy is obtained. Further improvement of fault location accuracy can be achieved by taking into account the distributed-parameter line model for lines of considerable length. Another means could be related to developing more effective filtering of distorted signals, and it seems that this task can be done with a well-designed neural network.

REFERENCES

[1] JOHNS A.T., AGGARWAL R.K., SONG Y.H., *Improved techniques for modelling fault arcs an faulted EHV transmission systems*, Generation, Transmission and Distribution, IEE Proceedings, Vol. 141 , No. 2, Mar. 1994, pp. 148–154.

[2] SAHA M.M., IŻYKOWSKI J., ROSOŁOWSKI E., *Fault Location on Power Networks*, Springer, London 2010.

[3] SAHA M.M., ROSOŁOWSKI E., IŻYKOWSKI J., *New Fault Location Method*, PACWorld, Vol. 21, September 2012.

[4] TAKAGI T., YAMAKOSHI Y., YAMAURA M., KONDOU R, MATSUSHIMA T., *Development of a new type fault locator using the one-terminal voltage and current data*, IEEE Trans. on Power Apparatus and Systems, Vol. 101, No. 8, Aug. 1982, pp. 2892–2898.